NUMERICAL ANALYSIS OF LEAN PREMIXED COMBUSTOR FUELED BY PROPANE-HYDROGEN MIXTURE

by

Mustafa Makhzoum Ali MAHJOUB[a*], Aleksandar M. MILIVOJEVIĆ[a], Vuk M. ADŽIĆ[a], Marija A. ŽIVKOVIĆ[b], Vasko G. FOTEV[a], and Miroljub M. ADŽIĆ[a]

[a] Faculty of Mechanical Engineering, University of Belgrade, Belgrade, Serbia
[b] Faculty of Mining and Geology, University of Belgrade, Belgrade, Serbia

Original scientific paper
https://doi.org/10.2298/TSCI160717131M

A numerical investigation of combustion of propane-hydrogen mixture in a swirl premixed micro gas turbine combustor is presented. The effects of hydrogen addition into propane on temperature distribution in the combustor, reaction rates of propane and hydrogen and NO_x emissions for different equivalence ratios and swirl numbers are given. The propane-hydrogen mixture of 90/10% by volume was assumed. The numerical results and measurements of NO_x emissions for pure propane are compared. Excellent agreements are found for all equivalence ratios and swirl numbers, except for the highest swirl number (1.13). It is found that the addition of hydrogen into propane increases NO_x emission. On the other hand, the increase of swirl number and the decrease of equivalence ratio decrease the NO_x emissions.

Key words: *swirl burner, premixed system, NO_x emissions*

Introduction

Reduction of emissions has been one of the major challenges and activities of researchers and engineers in combustion technologies. The use of hydrogen and hydrogen enriched fossil fuels appears to be an effective way to low carbon energy production. Besides, hydrogen is a renewable energy source, an energy storage medium and can be directly used in mixtures with natural gas and liquefied petrol gases (LPG) in existing gas piping and combustion systems [1-3]. Hydrogen is a clean, excellent fuel, which combustion product is water. Hydrogen production is based on a number of methods: use of solar, wind and nuclear energy, steam methane reforming, conversion of coal and biomass to hydrogen, water electrolysis, and others. Once produced, hydrogen is also considered a renewable energy. One should particularly pay attention to solar and wind energy for hydrogen production at competitive costs resulting from the fast technological developments. The main limitations of solar and wind power energy sources are site-specific operation, costs and intermittency [4, 5]. Regarding the intermittency problem, energy storage becomes very important and urgent issue [6]. Using batteries to store any energy surplus for later consumption can resolve the time mismatch between energy supply and demand. The shortcomings of battery storage are high priced, low-storage capacity, shorter equipment life, and considerable solid and wastes generated [7]. In order to better harness

* Corresponding author, e-mail: mosta752911@gmail.com

renewable energy, hydrogen has been identified as potential alternative fuel, as well as, energy storage carrier for the future energy supply [8, 9].

Hydrogen energy storage system presents an opportunity to increase the flexibility and resiliency of the sustainable energy supply system while potentially reducing overall energy costs on account of system integration and better utilization of renewable energy. On the other hand, its low density poses a storage problem [10]. Using pure hydrogen is possible, but not feasible in existing energy utilization systems. One of the possible solutions is hydrogen blending with other gaseous fuels. Blended hydrogen into the existing gas pipeline networks has been proposed as a means of increasing the output of renewable energy systems [11]. At relatively low concentrations of up to 10 vol.% hydrogen may be safely injected into existing fossil fuel gas pipeline systems with only minor modifications [12].

Realizing the growing importance of hydrogen, many researchers have focused their investigations on different aspects of its production and use. Nevertheless, in the available literature, there is a lack of published research on combustion of mixtures of LPG and hydrogen. Dutk *et al.* [13] performed an experimental investigation to study the emission characteristics of a novel low NO_x burner fueled by hydrogen rich mixtures with methane. The burner was tested in a cylindrical combustion chamber at atmospheric pressure. A burner thermal load of 25 kW and air-fuel equivalence ratio of 1.15 was maintained for various fuel compositions throughout the experimental tests. The investigation showed that lowest NO_x emissions were below 9 ppm and 14 ppm, at 3% of O_2 for 5% and 30% mass fraction of hydrogen in the fuel, respectively. The effect of hydrogen addition to ultra-lean counter flow methane/air premixed flame on the extinction limits and the characteristics of NO_x emissions were studied numerically by Guo *et al.* [14]. They indicated that the addition of hydrogen can significantly enlarge the flammable region and extend the flammability limit to lower equivalence ratios, and in constant equivalence ratio, the addition of hydrogen increases the emission of NO. Therkelsen *et al.* [15] implemented an experimental investigation to study the NO_x formation in hydrogen-fueled gas turbine engine. Three sets of fuel injectors were developed to facilitate stable operation while generating differing levels of air-fuel mixture non-uniformity. One set was designed to produce near uniform mixing while the others had differing degrees of non-uniformity. The higher emission of NO was found even with nearly perfect premixing when operated on hydrogen than when operated with natural gas. Choudhuri *et al.* [16] carried out an experimental investigation to study the characteristics of combustion and pollution of a diffusion flame in a vertical combustion chamber. The authors investigated a range of different fuel blends by varying the volumetric fractions of propane in the fuel mixture (5% up to 35 vol.%). They reported that the emission index of NO_x was 0.90 g/kg, at the baseline condition (95% hydrogen and 5% propane) which decreased to 0.34 g/kg, for 65-35% hydrogen/propane mixture. To the authors knowledge, there are no published papers on LPG/hydrogen mixture effects on NO_x emission for a swirl premixed micro gas turbine combustor.

The present paper focuses on numerical analysis of effects on swirl number and equivalence ratio on NO_x emission of a micro gas turbine combustor, fueled by 90/10 vol.% LPG/hydrogen mixture. The analysis was based on ANSYS Fluent commercial CFD package which was validated by comparing the available experimental data of the combustor and the numerical results. The analysis shows that the addition of hydrogen into LPG increases NO_x emissions.

Combustor model

The combustor, schematically given in fig. 1, consists of two components: combustor chamber and variable-length center body [17]. The combustor inner diameter is 66 mm

and the length 104 mm, the center body diameter is 25 mm, while the maximum length of the center body is 66 mm. The flat-vane swirler is mounted in the annular tube. Three swirlers with different vane angles of 30°, 45°, and 60° are used, corresponding to swirl numbers 0.45, 0.73, and 1.13, respectively. The center body and reaction chamber walls are water cooled, keeping the temperatures of the surfaces around 50 °C. The combustor is fueled by propane which nominal mass flow rate is 0.175 g/s, corresponding to nominal thermal power of P_0 = 8.1 kW

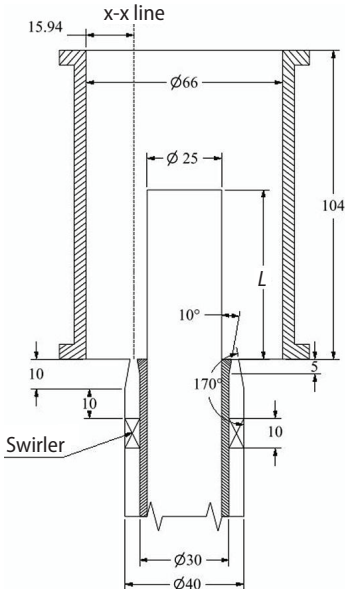

Figure 1. Schematics of mixing section and combustor

The air-fuel mixture is prepared in a mixing chamber and injected through a swirler into the combustor. The tests were performed at atmospheric conditions: pressure of 101.3 kPa and temperature of 20 °C. The tests were performed under parametric variations of equivalence ratio, swirl number and thermal power. The fuel and air-flow rates were measured using calibrated rotameters, while the exhaust gas composition was measured using Testo 350-XL and Testo 454 flue gas analyzers. To get representative flue gas samples and to prevent the outer air from interfering with exhaust gases, an extension tube with the same inner diameter and length as the combustor was attached to the combustor exit. The exhaust gas was sampled with a cooled stainless steel probe and transported through a heated tube to the gas analyzer. The accuracy of measurements is ±0.2% for O_2 and ±5% of reading for NO. The measured values of NO were corrected to 15% O_2 flue gas dry conditions.

Governing equations and boundary conditions

This numerical research is based on the ANSYS-Fluent software. The two equation, standard k-ε turbulence model is used. The generalized equation that governs the conservation of mass, momentum and energy, Reynolds averaged, can be written:

$$\frac{\partial}{\partial x_j}\left(\rho \bar{u}_j \bar{\beta} + \rho \overline{u_j' \beta'}\right) = \frac{\partial}{\partial x_j}\left(\Gamma_{\beta'} \frac{\partial \beta}{\partial x_j}\right) + \bar{\rho} S \beta \tag{1}$$

where $\Gamma_{\beta'}$ is the diffusion coefficient, S_β – the source term, and β – an arbitrary variable.

The local mass fraction of each species, Y_i is predicted through the solution of convection-diffusion conservation equation for the i^{th} species:

$$\frac{\partial(\rho Y_i)}{\partial t} + \bar{V}(\rho \vec{v} Y_i) = -\bar{V}\vec{j} + R_i + S_i \tag{2}$$

where S_i is the rate of creation by addition from the dispersed phase plus any user defined sources.

The net rate of production of species i due to reaction r is R_i given by smaller value of the two equations:

$$R_{i,\mathrm{r}} = v_{i,r}' M_{w,i} A \rho \frac{\varepsilon}{k} \min\left[\frac{Y_R}{v_{i,r}' M_{w,R}}\right] \tag{3}$$

$$R_{i,r} = v'_{i,r} M_{w,i} AB\rho \frac{\varepsilon}{k} \left[\frac{\sum_p Y_p}{\sum_i^N v''_{i,r} M_{w,i}} \right] \tag{4}$$

The emission of NO_x is calculated including both thermal and prompt NO_x. The effect of residence time (the Lagrangian reference frame concept) is included through the convection terms in the governing equations written on the Eulerian reference frame. For thermal and prompt mechanisms, only the species transport equation is needed:

$$\frac{\partial}{\partial x}(\rho Y_{NO}) + \overline{V}\left[\rho \vec{v} Y_{NO}\right] = \overline{V}\left[\rho D Y_{NO}\right] + U_{NO} \tag{5}$$

where D is the effective diffusion coefficient and U_{NO} is the source term.

The NO source term due to NO_x thermal mechanisms is:

$$U_{\text{termal,NO}} = M_{w,NO} \frac{\mathrm{d}[NO]}{\mathrm{d}t} \tag{6}$$

The prompt NO_x formation rate:

$$\frac{\mathrm{d}[NO]}{\mathrm{d}t} = f k'_{pr} [O_2]^a [N_2][FUEL] \mathrm{e}^{-E'_a / R_u T} \tag{7}$$

In the previous equation:

$$f = 4.75 + 0.0819n - 23.2\phi + 32\phi^2 - 12.2\phi^3 \tag{8}$$

$$k'_{pr} = 6.4x10^6 \left(\frac{RT}{P} \right)^{a+1} \tag{9}$$

where E'_a is the energy of activation, n – the number of carbon atoms per molecule, ϕ is the equivalence ratio, and a is the oxygen reaction order. The correction factor is a curve fit for experimental data [18].

The thermal NO_x formation rate is calculated by:

$$\frac{\mathrm{d}[NO]}{\mathrm{d}t} = k_{f,1}[O][N_2] + k_{f,2}[N][O_2] + k_{f,3}[N][OH] - k_{r,1}[NO][N] - k_{r,2}[NO][O] - k_{r,3}[NO][H] \tag{10}$$

In previous expression, $k_{f,1}$, $k_{f,2}$, and $k_{f,3}$ are the rate constant for the forward reaction and $k_{r,1}$, $k_{r,2}$, and $k_{r,3}$ are the corresponding reverse rate constants.

The specific heat, viscosity, and the thermal conductivity of the fluid mixture are calculated using the mass weighted average method. Second-order upwind scheme is used to discretize the governing equations, and the SIMPLE algorithm is used to deal with pressure-velocity coupling.

The boundary conditions are: the mass flow rate of propane is 0.175 g/s, and in the case of mixed (90% C_3H_8, 10% H_2 vol), 0.16915 g/s of C_3H_8 and 0.00085 g/s of H_2, which corresponds to thermal power of 8.1 kW. The mass flow rate of air corresponds to a chosen value of the equivalence ratio. The air-fuel mixture temperature at the combustor inlet is 20 °C. The radiation model is chosen to be discrete ordinates model. The temperature of the surface of combustor

walls is 50 °C. The combustor outlet pressure is assumed 101.3 kPa and the outlet temperature 20 °C. The swirl number and equivalence ratio are the independent variables.

The mesh

The combustion chamber domain as shown in fig. 2 is divided with maximum ortho skew of $1.988 \cdot 10^{-1}$ and a maximum aspect ratio of 8.81934. A mesh size, containing 339834 elements and 357345 nodes was found adequate for this simulation. The volume of the elements ranges from $1.202705 \cdot 10^{-10}$ m^3 to $2.0801 \cdot 10^{-9}$ m^3 for a total volume of $3.2332 \cdot 10^{-4}$ m^3, while face areas vary from $1.547025 \cdot 10^{-7}$ m^2 to $1.95281 \cdot 10^{-6}$ m^2.

The mesh independence has been checked as shown in tab. 1. It can be seen that the outlet temperature and velocity obtained by the mesh with medium size (339834 cells) is very close to that of fine mesh (502776 cells), as such, the medium size mesh is used.

Table 1. Mesh independence

Mesh	Number of nodes	Predicted temperature [K]	Percentage of change [%]	Predicted velocity [ms^{-1}]	Percentage of change [%]
Mesh-1	234337	1746.313	–	12.1912	–
Mesh-2	339834	1732.2	0.81	11.209	8.1
Mesh-3	502776	1726.4	0.3	11.0395	0.35

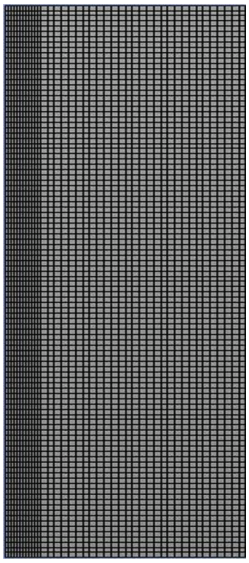

Figure 2. Computational mesh for the combustion chamber

Results and discussion

The variation of independent parameters of fuel composition, equivalence ratio and swirl number affects the NO_x emission, as follows.

Validation of the applied numerical analysis

For validation of the applied numerical analysis, results of experimental investigation of the micro gas turbine combustor, fueled by propane, are used [17]. The NO_x emission results of experimental and this numerical research, as a function of equivalence ratio and swirl number, are shown in fig. 3. It can be seen that predicted values of NO_x emissions agree very well with measured data for the equivalence ratios between 0.6 and 0.85, except for the highest value of swirl number (S = 1.13).

These findings of NO_x emission show that the applied numerical method can be used with a high level of confidence when burning pure propane. It can be assumed, therefore, that a similar level of confidence can be expected for numerical analysis of propane-hydrogen mixtures, at least for lower concentrations of hydrogen of up to 10 vol.%

As explained before, hydrogen can be directly used in existing LPG and natural gas pipelines and combustion systems with concentrations of up to 10 vol.% [11, 12]. Figure 4 shows the temperature distribution in combustor when pure propane and propane-hydrogen mixtures are used.

Figure 4 represents the mean temperature distribution along the central plane of combustor for equivalence ratio ϕ = 0.8 and different swirl numbers (0, 0.45, 0.73, and 1.13). It can be observed that by increasing the swirl number, the shape of high temperature zone changes, for flow with no swirl (S = 0) the flame is elongated, narrow, and protrudes out of the combustor. For the increase of the swirl number (0.73 and 1.13) the flame becomes wider, shorter and

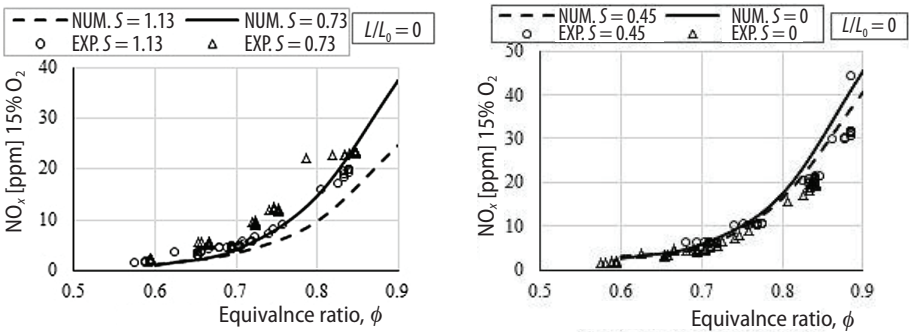

Figure 3. The NO_x emissions for different equivalence ratios and swirl numbers

ends inside the combustor for both fuels. The most pronounced difference between the flames of propane and propane-hydrogen mixture can be seen in $S = 1.13$. The flame of propane-hydrogen mixture is shorter and more compact than that of propane. This can be attributed to the increase of flame speed of the propane-hydrogen mixture.

Streamline pattern contours are plotted along a central plane of the combustion chamber for four swirl numbers (0, 0.45, 0.73, and 1.13) at equivalence ratio $\phi = 0.8$, as shown in fig. 5. The first noticeable observation is the presence of a central recirculation zone (CRZ) at the combustor inlet and wall recirculation zones (WRZ) in the burner corners. As the swirl number increases, the length of the WRZ decreases. This is due to the radial expansion of the flow

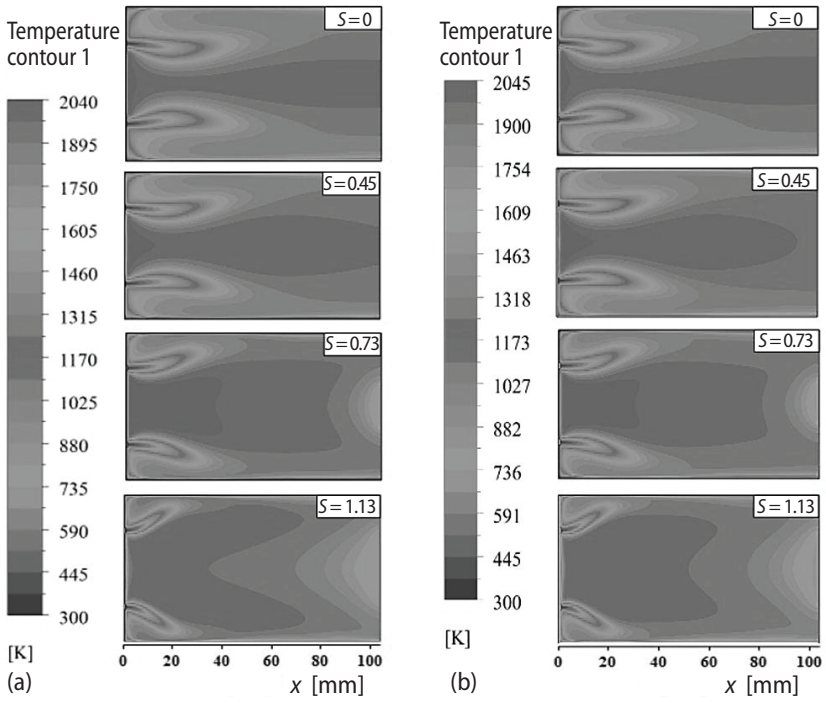

Figure 4. Temperature distributions along the central plane for $\phi = 0.8$, and different swirl numbers (a) pure propane, (b) 90 vol.% C_3H_8 and 10 vol.% H_2)

under the swirl effect. at no-swirling flow (S = 0) the CRZ is smaller compared to the size of the WRZ, as can be observed in this case, the length of CRZ is about 21 mm, while, the WRZ length is about 49 mm. For strong swirl number (S = 1.13), the flow structure is different and the size of the WRZ is reduced. Contrary to the size of WRZ the CRZ reaches a length of 75 mm, while the WRZ length decreases to 18 mm. Also, in cases of swirl numbers (0.73 and 1.13), it can be seen that re-circulation zone at the combustor outlet increases with S to the length of about 25 mm for (S = 1.13).

Figure 6 illustrates the temperature distribution along (x-x) line for swirl numbers (S = 0.45, 0.73, and 1.13) and equivalence ratio (ϕ = 0.8). It can be seen that in general, the increase of the swirl number moves the flame closer to the combustor inlet. For (S = 0.45) combustion zone protrudes out of the combustor outlet with the maximum temperature is at $x \geq 67$ mm. With the increase of the swirl number to 0.73, the maximum temperatures are at $x \geq 32$ mm. For the strongest swirl (S = 1.13), the combustion occurs inside the combustor, near the exit plane and the maximum temperature is at $x \geq 19$ mm.

The mass fraction profiles of C_3H_8 and H_2 and the reaction rates of propane-hydrogen flames at an equivalence ratio (ϕ = 0. 8) and swirl numbers 0.45, 0.73, and 1.13 are shown in figs. 7-9, respectively. The results show that the increase of swirl number leads to the decrease of distance for the consumption of both C_3H_8 and H_2. A noticeable difference between propane and hydrogen is faster consumption of hydrogen in general. The effect of swirl increase from 0.45 to 0.73 on fuel consumption is moderate, while for (S = 1.13) the rates of consumption have pronounced peaks.

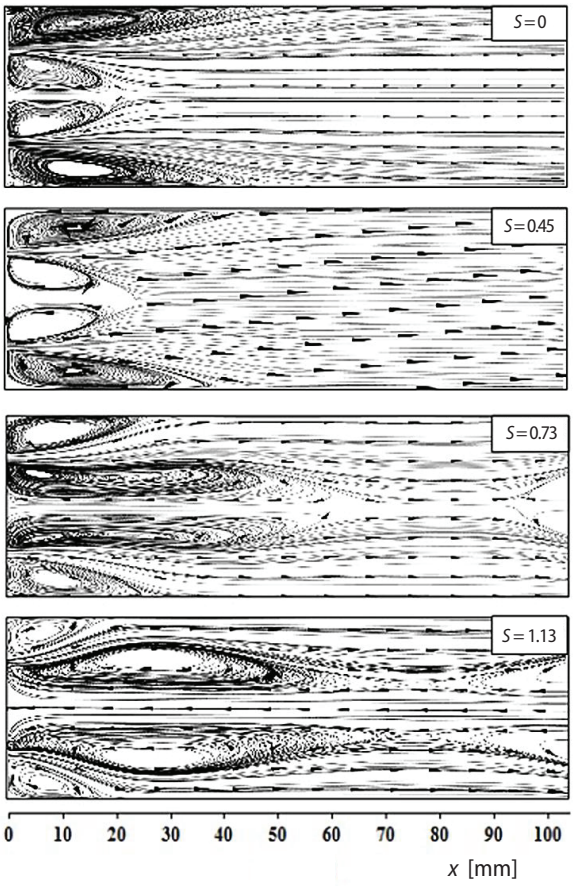

Figure 5. Flow structure along the central plane of combustor chamber for ϕ = 0.8, and different swirl numbers

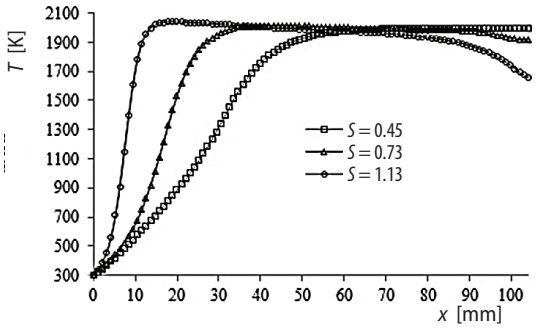

Figure 6. Temperature along (x-x) line; ϕ = 0.8 (propane/hydrogen mixture); different swirl numbers

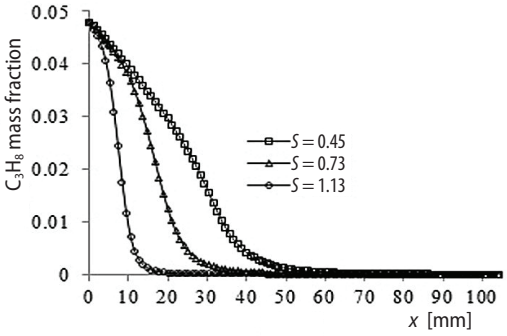

Figure 7. Propane mass fraction along (x-x); ϕ = 0.8 (propane/hydrogen mixture); different swirl numbers

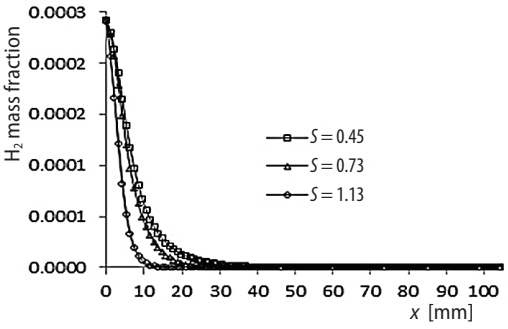

Figure 8. Hydrogen mass fraction along (x-x); ϕ = 0.8, (propane/hydrogen mixture); different swirl numbers

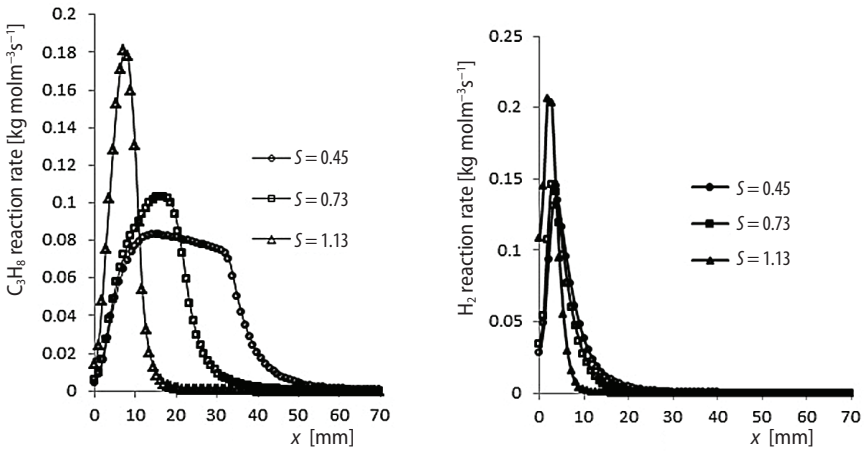

Figure 9. Reactions rates of propane and hydrogen along (x-x) line; ϕ = 0.8 (propane/hydrogen mixture); different swirl numbers

Figure 10 illustrates the variation of NO_x emissions for different equivalence ratios and swirl numbers when using pure propane and mixture of propane and hydrogen (90 vol.%

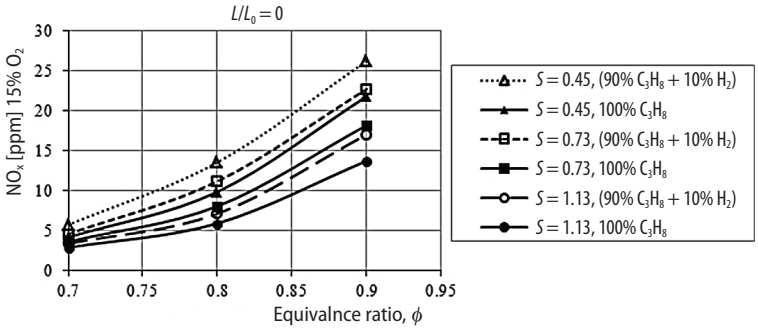

Figure 10. The NO_x emission for different equivalence ratios and swirl numbers of propane and propane/hydrogen mixture

C_3H_8+10 vol.% H_2). It can be clearly seen that the addition of hydrogen to propane increases NO_x emissions. This effect is smaller at lower equivalence ratios and increases with the increase of equivalence ratio. The maximum increase of NO_x takes place at equivalence ratio $\phi = 0.9$ for all cases of swirl numbers.

Conclusions

A numerical analysis of combustion of premixed propane air and propane-hydrogen air mixture was conducted. The temperature, reaction rates and concentrations of propane and hydrogen and NO_x emission were calculated over the range of equivalence ratios and swirl numbers for constant thermal power. The major conclusions of this work are as follows.

- For flow with no swirl the flame is elongated, narrow, and protrudes out of the combustor. The increase of swirl number moves the flame closer to the combustor inlet. The flame becomes wider, shorter and completely inside the combustor, for both fuels, due to the stronger re-circulation, induced by increased swirl. The most pronounced difference between the flames of propane and propane-hydrogen mixture can be seen for the highest swirl, $S = 1.13$. The flame of propane-hydrogen is shorter and more compact than that of propane. This can be attributed to the increase of flame speed of the propane-hydrogen mixture.
- The reaction rates of propane and hydrogen increase with the increase of swirl number, with pronounced peak for highest swirl, $S = 1.13$. A noticeable difference between propane and hydrogen is faster consumption of hydrogen.
- The addition of 10 vol.% of hydrogen into propane increases the NO_x emission by about 20% in equivalence ratio 0.9, and about 30% in equivalence ratio 0.9.
- The increase of swirl number from $S = 0.45$ to 1.13 lowers the NO_x emission between 30-40% for both fuels.

Nomenclature

A – empirical constant equal to 4.0, [–]
B – empirical constant equal to 0.5, [–]
D – effective diffusion coefficient, [kgm^{-3}s^{-1}]
d_h – swirler hub diamater, [m]
d_0 – swirler diamater, [m]
$E_a^{'}$ – activation energy, [Jmol^{-1}]
L – center body length, [m]
L/L_0 – normalized center body length, [–]
$M_{w,i}$ – molecular mass of species i, [kgmol^{-1}]
R_i – net rate of production of species i, [kgm^{-3}s^{-1}]
R_u – universal gas constant, (= 8.314), [Jmol^{-1}K^{-1}]
S – swirl number, $(= (2/3)\{[1-(d_h/d_0)^3]/[1-(d_e/d_0)^2]\}\tan\theta)$, [–]
S_i – rate of creation of species i , [kgm^{-3}s^{-1}]
T – temperature, [K]
t – time, [s]
U_{NO} – source term of NO, [ms^{-1}]
$\nu_{i,r}^{'}$ – stoichiometric coefficient for reactant i in reaction r, [–]
$\nu_{i,r}^{''}$ – stoichiometric coefficient for product i in reaction r, [–]
Y_i – mass fraction of species i , [–]
Y_P – mass fraction of any product species, [–]
Y_R – mass fraction of a particular reactant, [–]
x – reference for x-axis,

Greek symbols

ε – turbulent dissipation rate, [m^{2}s^{-3}]
θ – vane outlet angle, [°]
κ – turbulent kinetic energy per unit mass, [Jkg^{-1}]
μ – viscosity, [kgm^{-1}s^{-1}]
ρ – density, [kgm^{-3}]
ϕ – equivalence ratio, [–]

Subscripts

i – species, [–]
p – products, [–]
r – reactants, [–]

Acronymus

CRZ – central recirculation zone
WRZ – wall recirculation zones
LPG – liquefied petroleum gas

References

[1] Najjar, Y. S., Gaseous Pollutants Formation and their Harmful Effects on Health and Environment, *Innovative Energy Policies*, *1* (2011), ID E101203
[2] Tang, C., *et al.*, Progress in Combustion Investigations of Hydrogen Enriched Hydrocarbons, *Renewable and Sustainable Energy Reviews*, *30* (2014), Feb., pp. 195-216
[3] Nanthagopal, K., *et al.*, Hydrogen Enriched Compressed Natural Gas (HCNG): A Futuristic Fuel for Internal Combustion Engines, *Thermal Science*, *15* (2011), 4, pp. 1145-1154
[4] Ni, M., *et al.*, Potential of Renewable Hydrogen Production for Energy Supply in Hong Kong, *International Journal of Hydrogen Energy*, *31* (2006), 10, pp. 1401-1412
[5] Tabone, M. D., *et al.*, The Effect of PV Siting on Power System Flexibility Needs, *Solar Energy*, *139* (2016), Dec., pp. 776-786
[6] Riis, T., *et al.*, Hydrogen Production and Storage, International Energy Agency, Paris, 2006
[7] Chen, H., *et al.*, Progress in Electrical Energy Storage System: A Critical Review, *Progress in Natural Science*, *19* (2009), 3, pp. 291-312
[8] Morales, T. C., *et al.*, Hydrogen from Renewable Energy in Cuba, *Energy Procedia*, *57* (2014), Nov., pp. 867-876
[9] Levene, J. I., *et al.*, An Analysis of Hydrogen Production from Renewable Electricity Sources, *Solar Energy*, *81* (2007), 6, pp. 773-780
[10] Melaina, M., Eichman, J., Hydrogen Energy Storage: Grid and Transportation Services, Technical Report NREL/TP-5400-62518, U. S. Department of Energy, Washington DC, USA, 2015
[11] Melaina, M. W., *et al.*, Blending Hydrogen into Natural Gas Pipeline Networks: A Review of Key Issues, Technical Report NREL/TP-5400-62518, U. S. Department of Energy, Washington DC, USA, 2013
[12] Altfeld, K., Dave, P., Admissible Hydrogen Concentrations in Natural Gas Systems, Gas for Energy, Reprint ISSN 2192-158X, 2013, No. 3, pp.1-12
[13] Dutka, M., *et al.*, Emission Characteristics of a Novel Low Nox Burner Fueled by Hydrogen Rich Mixtures with Methane, *Journal of Power Technologies*, *95* (2015), 2, pp. 105-111
[14] Guo, H., *et al.*, The Effect of Hydrogen Addition on Flammability Limit and NOx Emission in Ultra-Lean Counterflow CH4/Air Premixed Flames, *Proceedings of the Combustion Institute*, *30* (2005), 1, pp. 303-311
[15] Therkelsen, P., *et al.*, Analysis of NOx Formation in a Hydrogen-Fueled Gas Turbine Engine, *Journal of Engineering for Gas Turbines and Power*, *131* (2009), 3, pp. 653-664
[16] Choudhuri, A., *et al*., Combustion Characteristics of Hydrogen-Propane Mixture, *ACS Division of Fuel Chemistry, 43* (1998), 1, pp. 107-110
[17] Adžić, M., *et al.*, Effect of a Microturbine Combustor Type on Emissions at Lean-Premixed Conditions, *Journal of Propulsion and Power*, *26* (2010), 5, pp. 1135-1143
[18] ***, Ansys, Inc. Theory Reference, Ansys Release 9.0,002114., 2004

Paper submitted: July 17, 2016
Paper revised: April 19, 2017
Paper accepted: May 25, 2017